

Control of As diffusion using ultrathin metal passivating layers at GaAs(100) surfaces

A. Raisanen, I. M. Vitomirov, and L. J. Brillson
Xerox Webster Research Center, Webster, New York 14580

P. D. Kirchner, G. D. Pettit, and J. M. Woodall
IBM T. J. Watson Research Center, Yorktown Heights, New York 10598

(Received 23 November 1992; accepted 8 March 1993)

We have performed low-energy cathodoluminescence spectroscopy (CLS) and synchrotron radiation photoemission (SXPS) measurements of Sb-passivated, clean and ordered molecular-beam epitaxy-grown GaAs(100) surfaces. SXPS measurements show an effective stabilization of the surface As/Ga atomic ratio under annealing for Sb-passivated surfaces, in contrast to the variations in the surface stoichiometry observed for unpassivated GaAs(100) surfaces. Our CLS data provide evidence for the generation of deep level states during annealing to 550 °C in the GaAs(100) subsurface region. Fabrication of a passivating layer by annealing a 2 ML Sb layer on the GaAs(100) surface has been found to dramatically reduce the formation of this subsurface defective layer by inhibiting As desorption from the surface. Studies of Al Schottky barrier formation on Sb-passivated layers demonstrate that the Schottky barrier value becomes independent of the details of processing, in contrast to the surface-dependent variations in barrier height observed for Al/GaAs(100) junctions without Sb passivating layers.

I. INTRODUCTION

Recently, there has been considerable experimental and theoretical interest in Sb overlayers on the surfaces of GaAs and other III-V semiconductors due to the epitaxially ordered nature of such overlayers.¹⁻³ Theoretical calculations have shown that ordered Sb layers will not introduce states in the GaAs(110) band gap,^{3,4} making possible the formation of interfaces with GaAs under flatband conditions. This effect is potentially useful for the control of interfacial interdiffusion, band bending, and Schottky barrier height for various metal/III-V systems.⁵ Thin ordered Sb layers have been recently investigated as passivating layers for InP(110)⁶⁻⁹ and GaAs(110)¹⁰⁻¹² surfaces, during both annealing^{7,8,11} and interface formation.^{6,9,12} Yamada *et al.*^{6,7} has investigated Sb passivation of InP(110) surfaces and has found evidence for a reduction in P desorption from the InP surface during annealing as well as removal of process-induced defects from the near-surface region. In addition, band bending induced by Sb deposition on both *n*- and *p*-type material is removed by annealing of the Sb layer, confirming that ordered Sb layers are capable of preserving flatband conditions at the semiconductor surface.^{6,7,10-12} Deposition of Ag⁶ on Sb-passivated *p*-InP(110) surfaces shows anomalously low band bending (≈ 0.5 eV reduction in $E_F - E_V$) compared to Ag/*p*-InP(110) surfaces without the Sb passivating layer, implying that the passivated surfaces exhibit substantially lower interface state densities. Yamada *et al.*⁹ has also investigated a variety of metal/InP(110) interfaces with and without annealed 1 ML Sb passivating layers and has found a general trend in which the Schottky barrier is lowered by Sb passivation of *p*-type InP(110) surfaces and increased on *n*-type InP(110) surfaces. Green *et al.*¹² has investigated In overlayers on Sb-passivated GaAs(110) surfaces and found that annealed Sb overlayers also are

effective in returning the GaAs(110) surface to flatband conditions. However, little effect on In-GaAs(110) reaction was observed, and only small changes in the In-induced band bending (≤ 0.15 eV) between passivated and unpassivated GaAs(110) surfaces were observed.

In this work we demonstrate that Sb overlayers can be used to successfully passivate molecular-beam epitaxy (MBE)-grown GaAs(100). We are able to show that ordered Sb overlayers can be used to stabilize the As/Ga stoichiometry of the GaAs(100) surface in a relatively narrow range by inhibiting the desorption of As from the surface. In contrast to the Sb/GaAs(110) cleaved surface results,¹⁰⁻¹² however, the annealed Sb overlayer is found to be incapable of forcing the surface to flatband conditions, presumably due to greater interface state densities and stronger E_F pinning in the MBE-grown material. We have also obtained direct evidence using low-energy cathodoluminescence for thermal processing-induced creation and annihilation of deep levels at the surface and in the near-surface region for clean GaAs(100) surfaces and surfaces passivated by Sb. We propose that these deep level states are mediated by the relative amount of As vacancies in the near-surface region versus As diffusion from the bulk to the surface. Sb passivating layers at the surface are found to be effective in reducing As desorption from the surface, allowing As vacancies to be annealed out, whereas unpassivated surfaces show a monotonic increase in deep level intensity with increasing annealing temperature. Finally, we demonstrate that ordered Sb passivating layers have a significant effect on the Schottky barrier formation of Al/GaAs(100) interfaces, forcing different GaAs(100) surfaces with substantially different thermal histories to form barriers similar to those formed at As-rich GaAs(100) surfaces.

II. EXPERIMENT

GaAs(100) specimens were grown by molecular-beam epitaxy (MBE) and capped with a thick ($> 1000 \text{ \AA}$) As layer by cooling the sample after growth in an As_4 flux. These specimens were then shipped under vacuum and de-capped in the analytical chamber by thermal desorption of the As layer. For As desorption and annealing, we placed the specimen rear face in direct contact with a Ta foil which acted as a resistive heating element, and controlled the sample temperature via an infrared pyrometer which was calibrated by a thermocouple in direct contact with the front face of a GaAs(100) test sample. All desorptions and anneals were held at the stated temperature for 5 min before cooling, and all spectroscopic measurements were performed at room temperature after the sample had cooled. Both the synchrotron radiation soft x-ray photoemission (SXPS) and low-energy cathodoluminescence (CLS) analytical chambers were equipped with fast cryopumps for efficient As removal during desorption.¹³ For SXPS, samples were placed at the common focus of a 6 m toroidal grating monochromator and a double pass cylindrical mirror electron energy analyzer. Angular-integrated electron energy distribution curves (EDCs) were acquired for the GaAs valence band, and As 3*d*, Ga 3*d*, Sb 4*d*, and Al 2*p* core levels. Our overall resolution, estimated by measuring the E_F cutoff of a thick Au film, was 0.15–0.3 eV in the photon energy range 22–100 eV. Surface photovoltage shifts were corrected for by determining the apparent Fermi energy cutoff of Al films grown on the GaAs(100) surface and comparing this value to the equilibrium E_F cutoff from an Au film grown on a grounded metal substrate.¹⁴ CLS measurements were performed by placing the samples at the common focus of an electronically chopped electron gun and the input optics of a Leiss single-pass prism monochromator. The luminescence signal excited from the sample by the electron beam was detected by a liquid-nitrogen-cooled Ge solid-state detector in the lock-in mode. Sb and Al metal overlayers were deposited by *in situ* evaporation from Ta or W coils. Metal coverages were monitored by a water-cooled quartz thickness monitor and are given in \AA or equivalent monolayers, with 1 ML of Sb corresponding to the GaAs(100) surface atomic density of $6.26 \times 10^{14} \text{ atoms/cm}^2$, such that 1 ML Sb = 1.91 \AA . The pressure during evaporation was maintained below 1×10^{-9} Torr, while the spectrometer operating pressure was below 2×10^{-10} Torr.

III. RESULTS

A. Surface chemical composition

For these experiments, SXPS was used to monitor the GaAs(100) surface composition and band bending. In Fig. 1(a) we show the As 3*d*/Ga 3*d* core level intensity ratio measured by SXPS at photon energies of 100 and 80 eV, respectively, which give roughly equivalent sampling depths for both core levels. After correction for photoelectric cross section differences between the As 3*d* and Ga 3*d* core levels,¹⁵ an As/Ga stoichiometry of unity corresponds to a measured As 3*d*₁₀₀/Ga 3*d*₈₀ ratio of approximately 0.8.

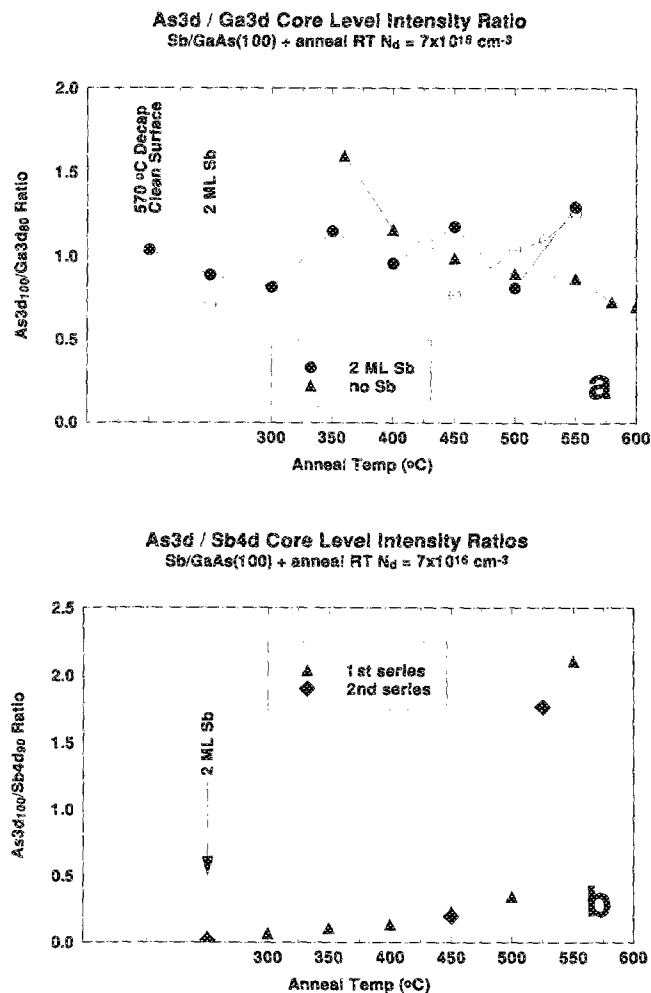
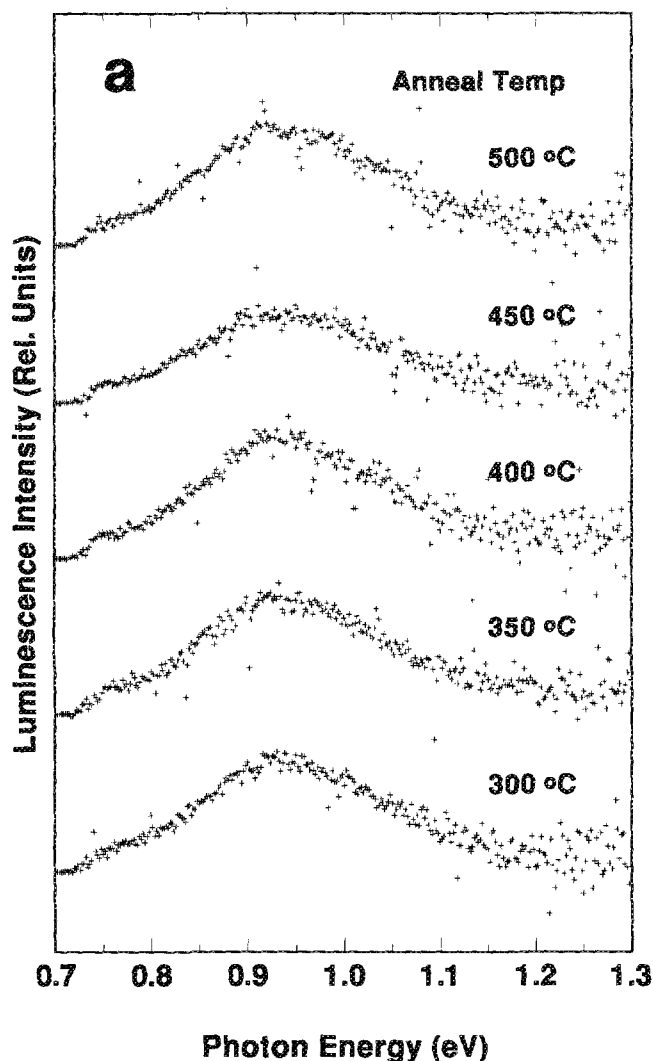


FIG. 1. (a) As 3*d*/Ga 3*d* core level intensity ratios from GaAs(100) surfaces as a function of processing and annealing temperature, taken at photon energies of 100 and 80 eV, respectively. Filled triangles represent the As 3*d*/Ga 3*d* ratio for a bare GaAs(100) surface as a function of annealing temperature, while the filled circles represent the As 3*d*/Ga 3*d* ratio with annealing for a GaAs(100) surface decapped at 570 °C which has had 2 ML Sb deposited upon it. Open circles represent a second set of anneals for the Sb-coated surface, where a second 2 ML Sb layer was deposited on the surface after annealing to 550 °C. (b) As 3*d*/Sb 4*d* core level intensity ratios from Sb/GaAs(100) interfaces as a function of annealing. Filled triangles represent the As 3*d*/Sb 4*d* ratio for a GaAs(100) surface initially decapped to 570 °C, upon which 2 ML Sb have been deposited. The filled diamonds represent the As 3*d*/Sb 4*d* ratio for the same surface which has had an additional 2 ML Sb deposited upon it after annealing to 550 °C.

The filled triangles represent the variation in As 3*d*/Ga 3*d* surface stoichiometry observed during annealing for a clean GaAs(100) surface without a Sb passivating layer.¹³ At each data point, the sample was held at the annealing temperature for 5 min. The filled circles represent the corresponding variation for a GaAs(100) surface which was first decapped and annealed for 5 min at 570 °C, then coated with 2 ML Sb, then sequentially annealed at the indicated temperatures for 5 min per data point. The open circles represent the As 3*d*/Ga 3*d* ratio for a second run of anneals of the same sample. After annealing to 550 °C, another 2 ML of Sb were deposited on the surface, and several anneals were repeated. In the no-Sb case, the de-

1 KeV Cathodoluminescence

Clean GaAs(100) RT $N_d = 7 \times 10^{16} \text{ cm}^{-3}$ 

1 KeV Cathodoluminescence

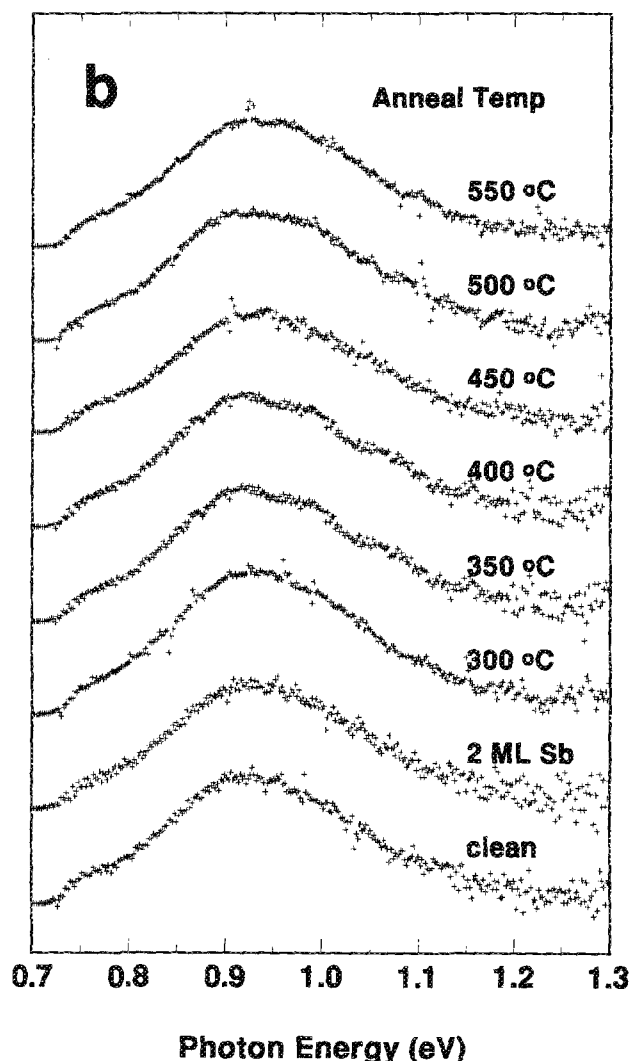
520 °C GaAs(100) RT $N_d = 7 \times 10^{16} \text{ cm}^{-3}$ 

FIG. 2. (a) Low-energy cathodoluminescence (CLS) of a clean GaAs(100) surface as a function of annealing temperature. The low doping level gives a relatively surface-sensitive measurement (Ref. 23). (b) CLS of a GaAs(100) surface with a 2 ML Sb passivation layer as a function of annealing temperature. The spectrum at bottom corresponds to the clean GaAs(100) surface, and the second spectrum from the bottom corresponds to the as-deposited (unannealed) Sb-coated GaAs(100) surface.

capped surface starts out highly As rich at low annealing temperatures (350 °C). As the bare GaAs(100) surface is annealed to higher temperatures, the As 3d/Ga 3d ratio decreases to approximately the stoichiometric value as excess As from the cap is desorbed. For annealing temperatures of 500 °C and above, the GaAs(100) surface exhibits a Ga-rich character, and at approximately 600 °C, the surface begins to decompose due to As desorption from the surface to the ambient vacuum, with the formation of visible Ga droplets on the surface.¹³

This variation in surface composition with annealing is substantially modified with the deposition of a thin Sb layer before the annealing cycle. The surface As 3d/Ga 3d

ratio exhibits only small variations about the stoichiometric value in the annealing temperature range 300–500 °C, and actually appears to increase slightly as the GaAs(100) surface is heated to 550 °C. When Sb is redeposited on this surface, the nearly stoichiometric GaAs(100) surface composition is recovered. The second set of anneals to 550 °C shows an As 3d/Ga 3d ratio variation similar to the first set.

In Fig. 1(b), we show the As 3d/Sb 4d ratio for the 2 ML Sb-covered 570 °C annealed GaAs(100) surface as a function of annealing temperature (filled triangles). The As 3d/Sb 4d ratio starts out very low for temperatures in the 300–500 °C range. For annealing temperatures above

500 °C, the As 3d/Sb 4d ratio increases by nearly a factor of 5. When a further 2 ML of Sb is deposited (filled diamonds), the As 3d/Sb 4d ratio returns to its low unannealed value, and increases with annealing temperature in good agreement with the first series of anneals.

B. Deep level emission

The existence and development of surface and bulk deep level states can be monitored by using CLS.¹⁶ In Fig. 2(a) we show CLS spectra for the clean *n*-GaAs(100) surface at a doping level of $7 \times 10^{16} \text{ cm}^{-3}$ Si. The surface was decapped at a temperature of 300 °C (bottom curve), and the CLS emission from the GaAs(100) surface at an incident electron energy of 1 keV was monitored as a function of annealing temperature. All measurements were obtained at room temperature (RT). We observe a broad luminescence peak centered about 0.93 eV photon energy for all annealing temperatures explored, and remarkably little change in the overall CLS deep level emission line shape or intensity. In Fig. 2(b) we show corresponding CLS spectra for a sample which has been capped by Sb. At bottom is the CLS emission from the clean GaAs(100) surface which has been annealed at 520 °C for 5 min. The next spectrum upwards shows the CLS emission from the same surface after 2 ML Sb have been deposited, and subsequent spectra show the effect on the deep level emission due to annealing. As was the case in the clean GaAs(100) surface, little or no variation is observed in the deep level emission intensity, position, or line shape as a function of processing. Corresponding spectra for a GaAs(100) surface decapped at only 300 °C before Sb passivation and annealing (not shown) display a similar lack of evolution as a function of annealing temperature.

A second set of GaAs(100) samples with a higher Si doping level were then investigated. In Fig. 3 we present CLS spectra obtained from such a highly doped sample ($1 \times 10^{19} \text{ cm}^{-3}$ Si). For the 350 °C decapped surface, there is a broad luminescence feature centered around 1.1 eV. As the surface is annealed to higher temperatures, this broad feature exhibits a systematic shift to lower photon energy, as well as a monotonic increase in intensity. There is also the appearance of a second deep level feature near 0.75 eV which appears as a shoulder to the low energy side of the main emission feature. This feature could be a discrete feature centered around 0.75 eV, but is more likely the high-energy end of emission below 0.7 eV, which is the energy cutoff of our Ge detector system.¹⁶ The overall increase in deep level emission intensity is a factor of 2 between 350 and 550 °C.

Figure 4 illustrates the modification in the deep level emission as a consequence of Sb deposition for surfaces decapped to two temperatures, 420 °C (a) and 530 °C (b). In section a, the clean 420 °C annealed GaAs(100) surface exhibits a broad deep level emission centered around 1.0 eV. Deposition of 2 ML of Sb causes the deep level emission to shift back to higher photon energy, so it appears generally similar to the lower-temperature annealed surfaces of Fig. 3. As this surface is annealed, the center of the deep level emission shifts to lower photon energy, but, in

1 KeV Cathodoluminescence

Clean GaAs(100) RT $N_d = 1 \times 10^{19} \text{ cm}^{-3}$

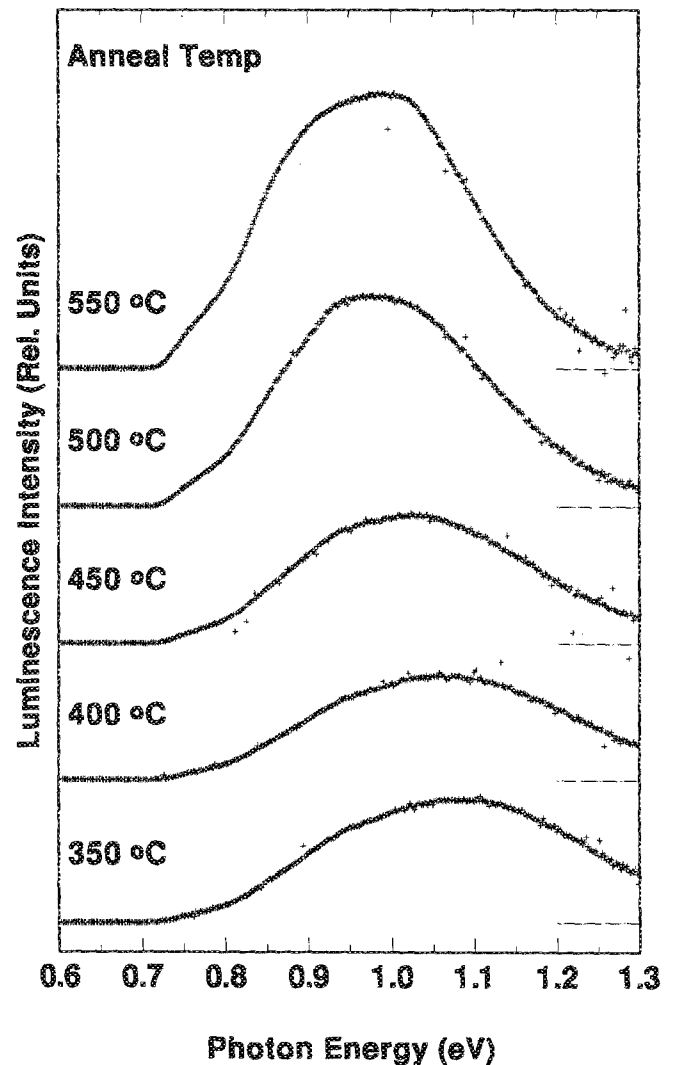


FIG. 3. CLS of a clean GaAs(100) surface as a function of annealing temperature. The high doping level of this sample results in a bulk-sensitive measurement (Ref. 23).

contrast to the results of Fig. 3, there is a systematic *decrease* in deep level emission intensity as the annealing temperature is increased, such that the overall deep level emission is reduced by a factor of 5 from the clean surface intensity after annealing to 550 °C. The small low-energy deep level feature observed in Fig. 3 at about 0.75 eV is observed in this case as well, and appears to increase slowly in intensity with increasing annealing temperature. In Fig. 4(b), we show corresponding spectra for a GaAs(100) surface initially decapped to 530 °C. Again, we have a broad deep level feature centered around 1.0 eV, which appears to be partially resolved into at least two main features. Deposition of Sb induces little change in the energy

1 KeV Cathodoluminescence
Sb/GaAs(100) RT $N_d = 1 \times 10^{19} \text{ cm}^{-3}$

1 KeV Cathodoluminescence
Sb/GaAs(100) RT $N_d = 1 \times 10^{19} \text{ cm}^{-3}$

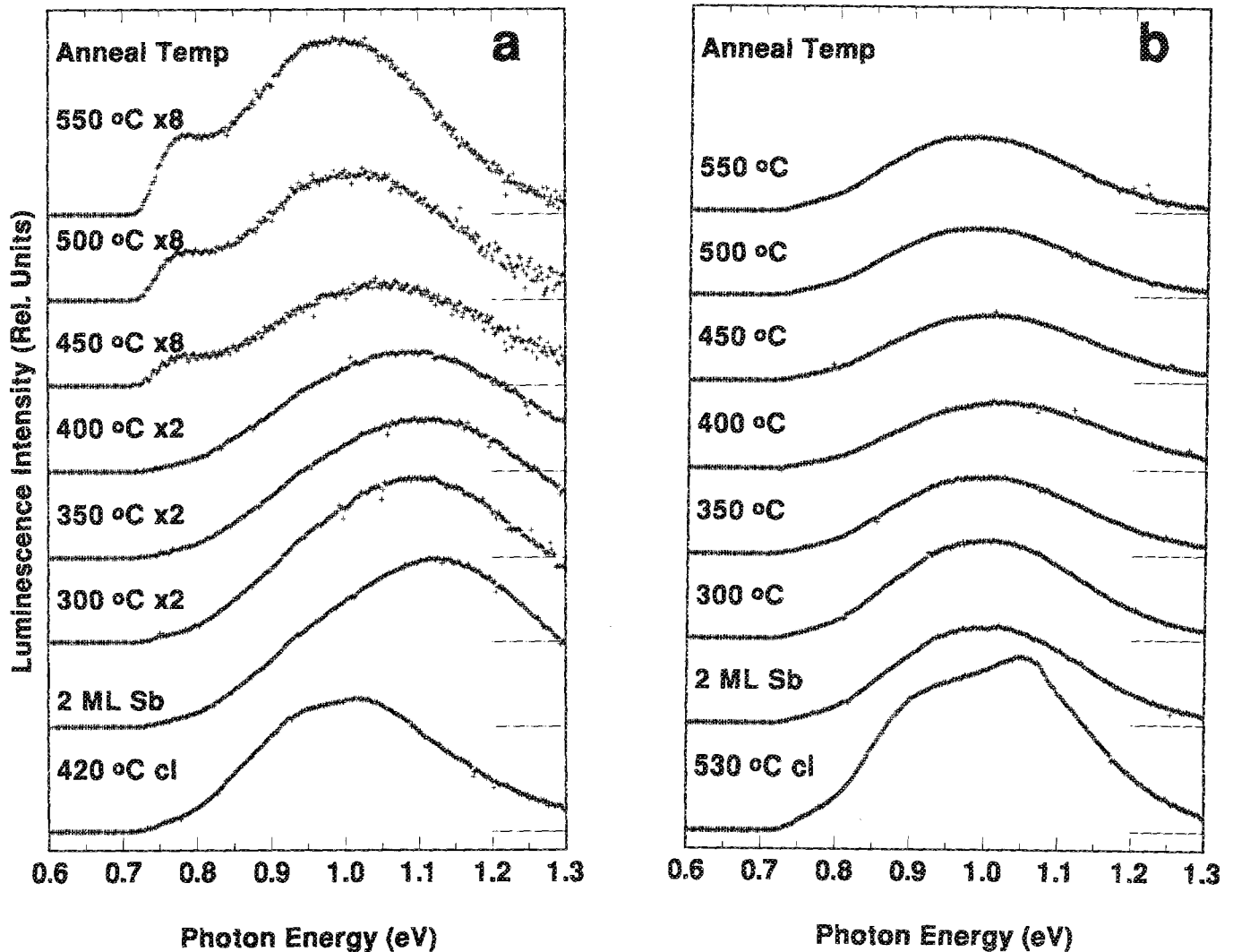


FIG. 4. (a) CLS for a Sb-passivated GaAs(100) surface as a function of annealing temperature. The bottom-most spectrum corresponds to the clean GaAs(100) surface after decapping at 420 °C (As-rich surface). The second-to-bottom spectrum corresponds to the GaAs(100) surface after deposition of 2 ML Sb but before annealing. (b) CLS for a Sb-passivated GaAs(100) surface as a function of annealing temperature. The bottom-most spectrum corresponds to the clean GaAs(100) surface after decapping at 530 °C (Ga-rich surface). The second-to-bottom spectrum corresponds to the GaAs(100) surface after deposition of 2 ML Sb but before annealing.

position of the deep level emission. Subsequent annealing reduces the overall deep level emission by only about 20%, with little or no apparent shift in the overall line shape. Also, once again the small low-energy shoulder is visible near 0.75 eV.

C. Fermi level movement

In Fig. 5 we illustrate the effect of the SXPS-determined E_F pinning position for Al/GaAs(100) junctions with and without annealed 2 ML Sb passivation layers. Filled triangles represent the evolution of the E_F pinning position for

350 °C (As-rich) GaAs(100) surfaces, and the open circles represent the corresponding measurement for 570 °C decapped (Ga-rich) GaAs(100) surfaces. The horizontal lines shown at 20 Å Al coverage represent the final E_F pinning positions observed for Al/GaAs(100) interfaces¹⁴ for surfaces decapped at 350 and 580 °C, respectively, corrected for the surface photovoltage shift as previously described. The two symbols near the 350 °C bare surface pinning position represent the final E_F pinning positions of the Sb-passivated surfaces after correction for the surface photovoltage shift. As shown in the figure, deposition of 2 ML Sb and annealing to 450 °C results in little change in

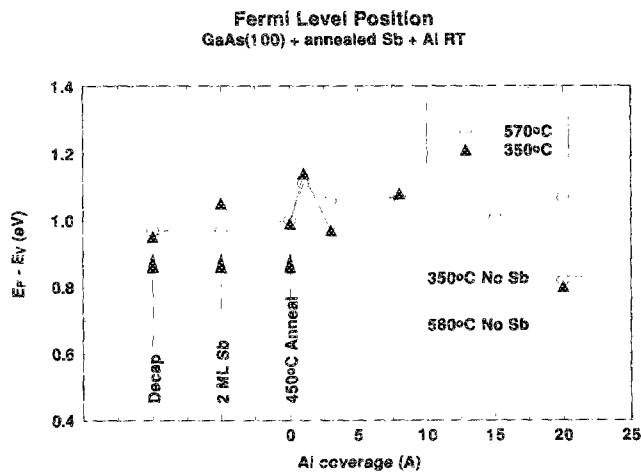


FIG. 5. E_F position of Al interfaces with Sb-passivated GaAs(100) surfaces as a function of Al coverage. Filled triangles correspond to the E_F position observed for a GaAs(100) surface initially decapped to 350 °C (As-rich surface), upon which 2 ML Sb were deposited and annealed to 450 °C before Al deposition. Open circles correspond to a GaAs(100) surface initially decapped to 570 °C (Ga-rich surface) under the same treatment. The isolated symbols at 20 Å Al coverage correspond to the final E_F positions observed for these surfaces after correction for the surface photovoltage shift. The horizontal tic marks correspond to the E_F pinning positions observed for Al/GaAs(100) interfaces without Sb passivation, which were initially decapped at the indicated temperature.

$E_F - E_V$ for either of the GaAs(100) surfaces. Deposition of Al causes a slight reduction in band bending, and the final value of $E_F - E_V$ after surface photovoltage (SPV) correction is found to be about 0.8 eV for both the low- and high-temperature annealed GaAs(100) surfaces, which corresponds to a n -type Schottky barrier height of 0.6 eV, in contrast to the finite 0.15 eV range in the Schottky barrier height which we observe between 350 and 580 °C decapped Al/GaAs(100) interfaces without Sb passivation layers.¹⁴

IV. DISCUSSION

A. Chemical composition and diffusion

Evidence for the inhibition of As desorption by the Sb passivating layer can be clearly seen in the behavior of the surface As 3d/Ga 3d ratio in Fig. 1(a). Deposition of a 2 ML Sb layer is effective in essentially eliminating the variation in As/Ga composition as a function of annealing temperature observed for the clean GaAs(100) surface (filled triangles),¹³ and in particular inhibits the loss of As from the surface that leads to a Ga-rich composition for annealing temperatures above 550 °C. The fact that re-depositing another 2 ML of Sb on the high-temperature annealed passivated surface leads to the same As 3d/Ga 3d ratio variation with subsequent annealing implies that little As has been lost from the surface by the temperature cycling. This effect could be due to Sb acting as a diffusion barrier to As movement from the surface into the vacuum, or the Sb layer acting as a "sacrificial" layer, desorbing in the place of As in order to form the Ga-rich (4×2)-c(8×2) surface. The excellent thermal stability of the Sb pas-

sivation layer is demonstrated in Fig. 1(b). For annealing temperatures below 500 °C, the As 3d/Sb 4d ratio is relatively low (<0.1), implying that the entire surface is well covered by a smooth layer of Sb with relatively little clustering or islanding. A small increase in the As 3d/Sb 4d ratio is observed as the annealing temperature is increased, which implies that small amounts of Sb are being removed from the surface by desorption. After the GaAs(100) surface is annealed to temperatures above 500 °C, the As 3d/Sb 4d ratio increases by a factor of 4 or more, indicating that most of the Sb overlayer has been desorbed. However, even at annealing temperatures as high as 550 °C, the observed As 3d/Ga 3d ratio implies that at least 0.5 ML of Sb remains at the surface. This result is consistent with previous studies of Sb/GaAs(110),¹⁰ where Sb layers in excess of 1 ML are easily desorbed by annealing, leaving a 1 ML Sb layer with high thermal stability. This high-stability layer has been described as acting as the outer layer of the semiconductor.¹⁰ Our low-energy electron diffraction (LEED) studies of the Sb/GaAs(100) interface support this interpretation. Sb appears to have a role at the surface very much like that of As; annealing the 2 ML Sb layer to a temperature of 300 °C produces a (1×1) reconstruction similar to that observed for a partially decapped GaAs(100) surface which still has several monolayers of elemental As on it.¹⁷ Further annealing in the 400–500 °C temperature range produces very clear LEED patterns characteristic of (2×4)-c(2×8) reconstructions,^{18–20} which are characterized by As dimers at the surface. This implies that Sb is substituting for As at these surfaces, forming dimer rows which are effective at inhibiting As outdiffusion and desorption from the surface. Annealing to 550 °C gives rise to a (4×2)-c(8×2) reconstruction, characteristic of Ga dimers at the surface.^{18–20} Most of the Sb has been desorbed at this point, suggesting that Sb at the surface is acting as a sacrificial layer, desorbing in the place of As at these high temperatures. The idea that little As has been removed by this process is supported by the fact that Sb can be redeposited on the high-temperature annealed surface, and a new series of anneals will reproduce the same surface stoichiometry and E_F pinning position as a function of temperature that the first set of anneals exhibited.

B. Deep level formation and band bending

Previous studies of Sb/GaAs(110) and Sb/InP(110) showed that deposition of Sb followed by annealing were sufficient to return both n and p -type semiconductor surfaces to near flatband conditions.^{6–11} Our SXPS results indicate that Sb deposition and subsequent annealing on the MBE-grown n -GaAs(100) surfaces used in this study do not force the surface to flatband conditions; rather, very little variation in E_F pinning position is observed. The small variations observed are of approximately the same range observed for our studies of decapped MBE-grown n -GaAs(100) surfaces without the presence of Sb,^{13,14} implying that the observed variation is driven by variations in the surface dipole^{21,22} as a function of surface reconstruction rather than by the annihilation of deep level states

which stabilize E_F . The minimal variation of $E_F - E_V$ as a function of annealing temperature in the presence of Sb overlayers suggests that the MBE-grown GaAs(100) surface is more strongly pinned than the cleaved GaAs(110) surface, and that the mechanism responsible for this pinning is substantially unaffected by Sb deposition and the resultant inhibition of As desorption and diffusion. We note that this is consistent with previous work^{3,4} which showed that Sb deposition on GaAs(110) does not introduce states in the gap that could modify the E_F position.

The CLS results presented in Figs. 2–4 provide clues as to the nature and spatial extent of diffusion and defect formation near the GaAs(100) surface during annealing, and how it is modified by the deposition of a Sb passivating layer. In Fig. 2 we see that very little variation in the intensity and line shape of the deep level emission is observed as a function of annealing in either the no-Sb case [Fig. 2(a)] or the case with 2 ML Sb on a Ga-rich 520 °C annealed surface [Fig. 2(b)]. Identical results were observed for As-rich 350 °C annealed surfaces with 2 ML Sb layers (not shown). The relatively low Si doping of this material, $7 \times 10^{16} \text{ cm}^{-3}$, means that the spectra of Fig. 2 are relatively surface sensitive.^{16,23} Earlier CLS results by our group¹³ show small variations in the CLS line shape as a function of annealing temperature and surface reconstruction, and variations of this order are observed in the spectra of Fig. 2; however, the absence of large variations in deep level emission observed under different thermal processing conditions implies that the surface region is relatively defect-free, with no large-scale generation of defects which could act as radiative recombination sites. This behavior is not significantly modified by the addition of a Sb passivating layer at the surface.

Figures 3 and 4 show CLS spectra taken on highly doped *n*-GaAs(100) surfaces, where the narrower depletion region renders this second set of measurements bulk sensitive relative to the results of Fig. 2.^{16,21} In contrast to the surface-sensitive results of Fig. 2, these spectra show marked evolution as a function of sample annealing and Sb deposition. In the case of no-Sb (Fig. 3), we observe the substantial creation of radiative recombination centers in the semiconductor bulk as the sample is annealed from 350–550 °C, as shown by the factor of 2 increase in overall deep level emission intensity and the shift of the line shape to lower photon energy. This increase could be due to the generation of As vacancies in the bulk during annealing, as As atoms diffuse from the bulk to the surface and are desorbed. The lack of variation of the CLS spectra in Fig. 2 suggests that As atoms lost from the near-surface region by desorption are rapidly replaced by diffusion of As atoms from the bulk, resulting in a relatively steady-state condition close to the surface. However, theoretical calculations²⁴ indicate that large-scale creation of As vacancies in the bulk is not thermodynamically favorable. The creation of Ga vacancies is thermodynamically favored,²⁴ but the decrease in overall As/Ga ratio as the annealing temperature of the pristine GaAs(100) is increased provides no evidence for Ga desorption.

The bulk-sensitive CLS measurements on very highly

Si-doped samples suggests a more complex set of defects is responsible for the increase in deep level emission for these surfaces. Recent experiments²⁵ have demonstrated that high concentrations of Si dopants can enhance self-diffusion in the GaAs lattice and that, under annealing, defect complexes, and reactions can be formed between As and Ga vacancies and Si atoms or clusters. For example, recent work by Suezawa *et al.*²⁵ propose that Si atoms can be transferred from one sublattice to the other by the reaction $\text{Si}_{\text{Ga}} + \text{V}_{\text{As}} \rightarrow \text{V}_{\text{Ga}} + \text{Si}_{\text{As}}$. A large variety of complex defects and reactions can be proposed to explain the present results. However, regardless of the details of such defect complexes, it is clear that As diffusion is closely coupled with the creation of the radiative recombination centers responsible for the deep level emission observed in Fig. 3 since the deposition of a 2 ML Sb layer at the surface can dramatically reduce the overall deep level emission intensity. Figure 4(a) shows a factor of 5 decrease in deep level emission intensity as the 420 °C decapped, Sb-coated GaAs(100) surface is annealed to 550 °C. In addition, the overall shift of the deep level emission line shape for the Sb-coated surface mirrors the energy shift for the no-Sb GaAs(100) surfaces, which suggests that the Sb layer is not directly inhibiting the defect reactions producing the deep levels of Fig. 3, but rather is hindering the loss of As from the surface that maintains the As vacancy concentration in the bulk. Once the desorption of surface As is reduced, As atoms diffusing from the bulk are available to annihilate As vacancies, so fewer As vacancies are available to react and form defect complexes. Interestingly, Fig. 4(a) shows a low-energy CLS feature near 0.75 eV which grows with annealing temperature despite the presence of Sb at the surface, which suggests the existence of a second defect complex creation process which does not depend on As vacancies.

Our interpretation of defect complex creation which is mediated by As vacancies is further supported by Fig. 4(b), which shows CLS spectra for a 530 °C decapped Sb-coated GaAs(100) surface. Only a 20% reduction in deep level emission is observed as the surface is annealed, and no shift of the line shape to lower photon energy is observed. In this case, it appears that either the defect complex reaction has proceeded nearly to completion at the initial As-desorption temperature of 530 °C, such that deposition of Sb and suppression of As outdiffusion has little effect; and/or that the reservoir of As atoms for annihilating As vacancies in the bulk has been depleted by the higher annealing temperature, such that little annihilation of As vacancies can take place.

The suppression of As desorption from the surface is found to have a significant effect on the Schottky barrier formation of Al/GaAs(100) interfaces. Figure 5 shows that the E_F pinning position for Al/*n*-GaAs(100) interfaces passivated by annealed Sb layers is identical to that of low-temperature annealed (350 °C) bare GaAs(100) surfaces,¹⁴ regardless of the actual initial As-decapping temperature of the surface. This clearly indicates that Sb is effective in reducing As desorption from the surface and actually forces all GaAs(100) surfaces, whether As rich or

Ga rich, to behave as if they are As rich. Again, this is consistent with the idea that the Sb passivation layer is suppressing As outdiffusion and that diffusion has a significant effect on the ultimate band bending.

V. CONCLUSIONS

We have demonstrated that Sb is able to form a well-ordered layer on GaAs(100) surfaces, just as it does on the GaAs(110) surface. In addition, this layer is remarkably stable, with more than 0.5 ML remaining at the surface for annealing temperatures as high as 550 °C. Our SXPS and CLS results clearly demonstrate that Sb efficiently caps the GaAs(100) surface against As loss from the surface under annealing, and thus allows the removal of As vacancies by As diffusion from the bulk, which is effective in removing defective subsurface layers of the semiconductor. We observe the greatest reduction in deep level emission for GaAs(100) surfaces decapped at relatively low temperatures, possibly implying the presence of a subsurface As reservoir which acts to eliminate As vacancies, but which is depleted by high-temperature anneals. The effect of the Sb passivation layer on the Schottky barrier value is relatively small, but clearly forces even highly Ga-rich surfaces to behave as As-rich surfaces, reinforcing the idea that the Sb layer acts as a sacrificial layer against reaction. The use of Sb passivation layers at GaAs(100) surfaces offers a method of improving the process latitude for the thermal processing of GaAs(100) surfaces, as reproducible As-rich surface stoichiometries and reconstructions can be obtained over a wide range of initial annealing temperatures and reconstructions.

ACKNOWLEDGMENTS

The authors gratefully acknowledge partial support by the Office of Naval research under Contract No. N00014-91-C-0037. Synchrotron radiation photoemission spectroscopy was performed at the University of Wisconsin Synchrotron Radiation Center, supported by the National Science Foundation.

¹P. Skeath, I. Lindau, C. Y. Su, and W. E. Spicer, *J. Vac. Sci. Technol.* **17**, 874 (1980).

- ²P. Martensson and R. M. Feenstra, *Phys. Rev. B* **39**, 7744 (1989).
³C. Mailhot, C. B. Duke, and D. J. Chadi, *Phys. Rev. Lett.* **53**, 2114 (1984); *Phys. Rev. B* **31**, 2213 (1985).
⁴C. M. Barton, C. Calandra, F. Manghi, and E. Molinar, *Phys. Rev. B* **27**, 1251 (1983).
⁵L. Brillson, *Surf. Sci. Rep.* **2**, 123 (1982).
⁶M. Yamada, A. K. Wahi, P. L. Meissner, A. Herrera-Gomez, T. Kendelewicz, and W. E. Spicer, *Appl. Phys. Lett.* **58**, 2243 (1991).
⁷M. Yamada, C. J. Spindt, K. E. Miyano, P. L. Meissner, A. Herrera-Gomez, T. Kendelewicz, and W. E. Spicer, *J. Appl. Phys.* **71**, 314 (1992).
⁸M. Yamada, A. M. Green, A. Herrera-Gomez, T. Kendelewicz, and W. E. Spicer, *Jpn. J. Appl. Phys.* **30**, 1982 (1991).
⁹M. Yamada, A. K. Wahi, T. Kendelewicz, and W. E. Spicer, *Appl. Surf. Sci.* **56-58**, 325 (1992).
¹⁰F. Schaffler, R. Ludeke, A. Taleb-ibrahim, G. Huges, and D. Rieger, *J. Vac. Sci. Technol. B* **5**, 1048 (1988).
¹¹R. Cao, K. Miyano, T. Kendelewicz, I. Lindau, and W. E. Spicer, *Surf. Sci.* **206**, 413 (1988).
¹²A. M. Green, M. Yamada, T. Kendelewicz, A. Herrera-Gomez, and W. E. Spicer, *J. Vac. Sci. Technol. B* **10**, 1918 (1992).
¹³I. M. Vitomirov, A. D. Raisanen, A. C. Finnefrock, R. E. Viturro, L. J. Brillson, P. D. Kirchner, G. D. Pettit, and J. M. Woodall, *J. Vac. Sci. Technol. B* **10**, 1898 (1992).
¹⁴A. Raisanen, I. Vitomirov, L. J. Brillson, P. D. Kirchner, G. D. Pettit, and J. M. Woodall, *Proceedings of the 20th International Conference on the Physics and Chemistry of Semiconductor Interfaces* (to be published).
¹⁵J. J. Yeh and I. Lindau, *At. Data Nucl. Data Tables* **32**, 1 (1985).
¹⁶L. J. Brillson and R. E. Viturro, *Scanning Microsc.* **2**, 789 (1988).
¹⁷R. Z. Bachrach, R. S. Bauer, P. Chiaradia, and G. V. Hansson, *J. Vac. Sci. Technol.* **19**, 335 (1981).
¹⁸M. D. Pashley, K. W. Haberern, W. Friday, J. M. Woodall, and P. D. Kirchner, *Phys. Rev. Lett.* **60**, 2176 (1988).
¹⁹M. D. Pashley, *Phys. Rev. B* **40**, 10481 (1989).
²⁰D. K. Biegelson, R. D. Bringans, J. E. Northrup, and L.-E. Swartz, *Phys. Rev. B* **41**, 5701 (1990).
²¹W. Chen, M. Dumas, D. Mao, and A. Kahn, *J. Vac. Sci. Technol. B* **10**, 1886 (1992).
²²R. Duszak, C. J. Palmström, L. T. Florez, Y.-N. Yang, and J. H. Weaver, *J. Vac. Sci. Technol. B* **10**, 1891 (1992).
²³The depth sensitivity of the high versus low-doped GaAs(100) samples was tested experimentally by comparing HeNe laser-excited photoluminescence (PLS) and CLS spectra obtained from the same surfaces. PLS should have a much greater bulk sensitivity than CLS, since the penetration depth of 1.96 eV photons is much greater than that of 1 keV electrons. We found substantial differences between PLS and CLS spectra for low-doped samples, whereas the PLS and CLS measurements were essentially identical for highly doped samples, thus confirming that high doping levels result in a bulk-sensitive measurement.
²⁴S. B. Zhang and J. E. Northrup, *Phys. Rev. Lett.* **67**, 2339 (1991).
²⁵M. Suezawa, A. Kasuya, Y. Nishina, and K. Sumino, *J. Appl. Phys.* **69**, 1618 (1991).